Catalysis Today 164 (2011) 234–239

Contents lists available at ScienceDirect

Catalysis Today

journal homepage: www.elsevier.com/locate/cattod

The effect of support reducibility on the stability of Co/CeO_2 for the oxidative steam reforming of ethanol

Adriana M. da Silva[a], Kátia Regina de Souza[a], Lisiane V. Mattos[b], Gary Jacobs[c], Burtron H. Davis[c], Fábio B. Noronha[a,*]

[a] Instituto Nacional de Tecnologia - INT, Av. Venezuela 82, CEP 20081-312 Rio de Janeiro, Brazil
[b] Departamento de Engenharia Química, Programa de Pós-Graduação em Engenharia Química, Universidade Federal Fluminense, Rua Passos da Pátria 156, Niterói, Brazil
[c] Center for Applied Energy Research, The University of Kentucky, 2540 Research Park Drive, Lexington, KY 40511, USA

ARTICLE INFO

Article history:
Available online 4 November 2010

Keywords:
Hydrogen production
Ethanol oxidative steam reforming
Co/CeO_2 catalyst
Deactivation mechanism

ABSTRACT

Ceria plays an active catalytic role in removing carbon from the catalyst by a support-mediated cleaning mechanism. Increasing the support surface area using a novel preparation method led to improved catalyst stability and a lower coking rate. DRIFTS of adsorbed ethanol shows that oxygen from the support facilitates the formation of acetate intermediate species, thus demonstrating the ability of the support to donate oxygen. This oxygen may come from either O adatoms by adsorption of O_2 at vacancies, whereby the cerium atoms involved are Ce^{4+}. Or, it may come from vacancy-associated Type II bridging OH groups, where the cerium atoms involved are Ce^{3+}. The higher oxygen/OH group mobility of high ceria surface area promotes the mechanism of carbon removal, which in turn contributes to the high stability of Co/CeO_2 catalyst.

1. Introduction

Co-based catalysts have been extensively studied for hydrogen production through steam reforming (SR) [1–3], partial oxidation (POX) [4] and oxidative steam reforming (OSR) [5,6] of ethanol. However, the design of effective catalysts for these reactions remains a significant challenge from the standpoint of attaining catalyst stability. Catalyst deactivation during ethanol conversion reactions is generally attributed to Co particle sintering [7], carbon deposition [8–10] and oxidation of Co metallic particles [5].

Two types of carbonaceous deposits are reported on supported Co catalysts: filamentous carbon and amorphous carbon covering the metallic particle and the support [8–10]. The nature of carbon formed depends on both the reaction temperature and the nature of the support selected.

Severe deactivation was observed on Co-based catalysts during SR at low temperature (below 773 K), due to the Co particle encapsulation by an amorphous carbon layer [9–11]. When the reaction was carried out at high temperatures (above 773–873 K), carbon filaments were detected but the catalyst remained quite stable [9–11]. Above 873 K, carbon deposits were no longer detected, and this was attributed to the removal of carbon from the surface of the metal by the reverse Boudouard reaction.

The support reducibility plays an important role in defining the stability of supported catalysts during SR of ethanol. Redox supports like ceria and ceria-containing mixed oxides have been proposed to improve catalyst stability due to their high oxygen storage capacities [12,13].

Ir/CeO_2 catalyst was quite stable during SR of ethanol at 923 K and low space velocity [12]. According to the authors, ceria activates H_2O and produces oxygen, which is transferred from ceria to Ir to oxidize carbon species, maintaining the metal surface clean. Song and Ozkan [7] studied the SR of ethanol over Co/ZrO_2, Co/CeO_2 and $Co/CeZrO_2$. Co/ZrO_2 and $Co/CeZrO_2$ catalysts deactivated during reaction whereas Co/CeO_2 remained stable for 45 h. The following stability order was observed: $Co/ZrO_2 < Co/CeZrO_2 < Co/CeO_2$. They proposed that oxygen from the support oxidizes the deposited carbon, thereby improving catalyst stability. However, in general, $CeZrO_2$ materials display much higher oxygen storage capacity (OSC) than ceria and thus, one would expect that $Co/CeZrO_2$ catalyst should exhibit higher stability relative to Co/CeO_2, which did not happen. Therefore, the previous studies in the literature [7] regarding the exact role of oxygen mobility on the stability of Co-based catalysts during SR of ethanol are suggestive, but not conclusive.

However, there are no studies about the precise role of oxygen mobility and its impact on the stability of Co-based catalysts for OSR of ethanol. In addition, the oxidation of metallic particles by oxygen from the feed is another potential cause of catalyst deactivation in the case of OSR. Pereira et al. [5] studied the performance of Co/SiO_2, $Co\text{-}Rh/SiO_2$ and $Co\text{-}Ru/SiO_2$ catalysts during OSR. They observed a decrease in ethanol conversion that was accompanied by a decrease

* Corresponding author. Tel.: +55 21 2123 1177; fax: +55 21 2123 1166.
E-mail address: fabio.bellot@int.gov.br (F.B. Noronha).

0920-5861/$ – see front matter © 2010 Elsevier B.V. All rights reserved.
doi:10.1016/j.cattod.2010.10.033

in hydrogen selectivity and an increase in acetaldehyde selectivity. They proposed that the loss of activity of Co-based catalysts was due to the oxidation of the surface of Co particles by oxygen from the feed. On bimetallic catalysts, the addition of a noble metal (e.g., Rh, Ru) was proposed to stabilize the Co in a reduced state (i.e., the proposed active state phase for SR), preventing oxidation of the cobalt particles.

The aim of this work was to investigate the role of lattice oxygen on the stability of ceria supported Co-catalysts with different OSC during OSR of ethanol.

2. Experimental

2.1. Catalyst preparation

Cerium oxide was prepared by two different methods: (i) calcination of cerium (IV) ammonium nitrate at 1073 K (CeO_2-LS); and (ii) addition of an aqueous solution of cerium (IV) ammonium nitrate to an ammonium hydroxide solution while the pH was maintained in the range of 10–14 [14]. In the later case, after precipitation, the material was heated to 369 K and held at this temperature for 96 h. The precipitate was collected by centrifugation. Finally, the material was washed until the filtrate reached a pH of 7 and dried at 393 K for 12 h. Then, the sample was calcined at 773 K (1 K/min) for 12 h (CeO_2-HS). Cobalt (10 wt.%) was added to the CeO_2 support by incipient wetness impregnation using an aqueous solution of $Co(NO_3)\cdot 6H_2O$. After impregnation, the samples were calcined at 673 K for 2 h.

2.2. BET surface area

The BET surface areas of the samples were measured using a Micromeritics ASAP 2000 analyzer by nitrogen adsorption at the boiling temperature of liquid nitrogen.

2.3. X-ray Diffraction (XRD)

XRD measurements were recorded using a RIGAKU diffractometer employing CuK_α radiation ($\lambda = 1.5406$ Å). Data were collected between $2\theta = 25^\circ$ and 75° (0.04°/step; 1 s/step). The Scherrer equation was used to estimate the ceria crystallite mean diameter.

2.4. Oxygen storage capacity (OSC)

Oxygen storage capacity measurements were carried out on Co/CeO_2-LS and Co/CeO_2-HS catalysts in a multipurpose unit connected to a quadrupole mass spectrometer (Balzers, Omnistar). The samples (100 mg) were reduced under H_2 at 1023 K for 1 h. Then, the samples were cooled to 723 K and a 5% O_2/He mixture was passed through the catalyst until the uptake of oxygen was complete. The reactor was purged with He and the dead volume was obtained by switching the gas to the 5% O_2/He mixture. Finally, the amount of oxygen consumed on the catalysts was calculated by taking into account a previous calibration of the mass spectrometer.

2.5. Diffuse reflectance infrared spectroscopy (DRIFTS)

DRIFTS spectra were recorded using a Nicolet Nexus 870 spectrometer equipped with a DTGS-TEC detector. A Thermo Spectra-Tech cell capable of high pressure/high temperature operation and fitted with ZnSe windows served as the reaction chamber for in situ adsorption and reaction measurements. Scans were taken at a resolution of 4 to give a data spacing of 1.928 cm^{-1}. The number of scans taken was 512. The amount of catalyst was ~40 mg.

The cobalt oxide particles are completely reduced only at high temperature (1023 K), which may not be reached by the Thermo Spectra-Tech cell heated under H_2. Therefore, samples were first pre-reduced in an external fixed bed reactor by ramping in 200 mL/min H_2:He (1:1) at ~10 K/min to 1023 K, holding at this temperature for 1 h, and cooling to room temperature, whereby the gas flow was switched to 1% O_2/He (25 mL/min) for 4 h for passivation. Samples were re-reduced in situ by ramping in 200 mL/min H_2:He (1:1) at ~10 K/min and holding at 773 K for 1 h. The catalyst was purged in flowing He at 773 K, prior to cooling in flowing He to 313 K.

For ethanol adsorption tests, He was bubbled at ~15 mL/min through a saturator filled with ethanol and held at 273 K. For OSR, 15 mL/min of ~0.75% O_2/He was bubbled through the H_2O saturator held at 298 K and another 15 mL/min of He was bubbled through an ethanol saturator held at 273 K. The H_2O/ethanol molar ratio obtained was 2.0, while the O_2/ethanol molar ratio was 0.5. The two streams were combined at a tee-junction, prior to which 1 psig check valves were added to prevent the possibility of back-flow. Adsorption/reaction measurements were started at 323 K, and then the temperature was increased at 10 K/min; measurements were recorded at 373, 473, 573, 673 and 773 K.

2.6. TG analysis

TPO experiments were performed using a TA Instruments TGA analyzer (SDT Q 600) in order to determine the amount of carbon formed over the catalyst. Approximately 10 mg of spent catalyst was heated under air flow from room temperature to 1173 K at a heating rate of 20 K/min and the weight change was measured.

2.7. Reaction conditions

OSR was performed in a fixed-bed reactor at atmospheric pressure, using a mass of catalyst of 20 mg. Prior to reaction testing, catalysts were reduced at 1023 K, for 1 h and then purged under N_2 at the same temperature for 30 min. All reactions were carried out at 773 K. The H_2O/ethanol molar ratio was 3.0, while the O_2/ethanol molar ratio was 0.5. The reactant mixtures were obtained using two saturators containing water and ethanol, which were maintained at the temperatures required to obtain the desired H_2O/ethanol and O_2/ethanol molar ratios. The reactant mixture was obtained by flowing 5.6 vol.% O_2 in N_2 (28 mL/min) and N_2 (32 mL/min) streams through each saturator containing ethanol and water, respectively.

In order to observe the catalyst deactivation within a short timeframe, a small amount of catalyst was used (20 mg). The samples were diluted with inert SiC (SiC mass/catalyst mass = 3.0) with the bed height being around 3 mm.

The reaction products were analyzed by gas chromatography (Micro GC Agilent 3000 A) containing two channels for dual thermal conductivity detectors (TCD) and two columns: a molecular sieve and a Poraplot U column. The ethanol conversion ($X_{ethanol}$) and product distribution (S_x) were determined from:

$$X_{ethonol} = \frac{(n_{ethonol})_{fed} - (n_{ethonol})_{exit}}{(n_{ethonol})_{fed}} \times 100 \quad (1)$$

$$S_x = \frac{(n_x)_{produced}}{(n_{total})_{produced}} \times 100 \quad (2)$$

where $(n_x)_{produced}$ = moles of x produced (x = hydrogen, CO, CO_2, methane, acetaldehyde or ethylene) and $(n_{total})_{produced}$ = moles of H_2 + moles of CO + moles of CO_2 + moles of methane + moles of acetaldehyde + moles of ethylene (the moles of water produced are not included).

3. Results and discussion

3.1. Catalyst characterization

The BET surface area of CeO_2-HS support (225 m^2/g) was much higher than that obtained for CeO_2-LS support (14 m^2/g). The addition of Co to the support does not result in significant changes to the BET surface area of both samples.

The average domain size estimated by Scherrer line broadening analysis for CeO_2-HS support (2 nm) was found to be much smaller than that of the CeO_2-LS support (21 nm). The OSC of the Co/CeO_2-HS catalyst (1539 μmol O_2/g_{cat}) was higher than that of Co/CeO_2-LS (1130 μmol O_2/g_{cat}). This result revealed a higher density of oxygen vacancies sites for Co/CeO_2-HS as a result of the higher oxygen mobility of the high ceria surface area.

Fig. 1a–d shows the IR spectra of adsorbed ethanol for Co/CeO_2-LS and Co/CeO_2-HS catalysts at different temperatures. The DRIFTS spectra collected at room temperature exhibited bands at 1049, 1087, 1356, 1406, 1444, 2862, 2925 and 2969 cm^{-1} for Co/CeO_2-LS (Fig. 1a) and at 1122, 1172, 1381, 1400, 1454, 2867, 2929, 2977 cm^{-1} for Co/CeO_2-HS (Fig. 1c). These bands correspond to different vibrational modes of ethoxy species formed from ethanol dissociation over Ce cations [15,16]. For Co/CeO_2-LS catalyst, there are additional bands at 1265, 1624 and 1892 cm^{-1}, which are consistent with molecularly adsorbed ethanol [17], the ν(CO) vibrational mode of acetyl species [17], and the ν(CO) stretching mode of bridge-bonded CO adsorbed on Co particles [18], respectively. In addition to these bands, DRIFTS spectra revealed the presence of bands corresponding to the different vibrational modes of acetate species (1454 and 1554 cm^{-1}) [16] on Co/CeO_2-HS catalyst whereas these bands were not detected for the Co/CeO_2-LS catalyst. According to the reaction mechanism proposed in the literature [19], ethanol adsorbs dissociatively producing ethoxy species, which are further oxidized to acetate species. Since there is no oxygen in the feed, the oxidation of ethoxy into acetate species must be supplied by oxygen from the support and involves surface O from either O adatoms or surface OH groups. It has been reported in the literature [20] that acetate species are formed via two reaction pathways: (i) the reaction between the acetyl species and oxygen from the support and/or (ii) the reaction of acetaldehyde with sur-

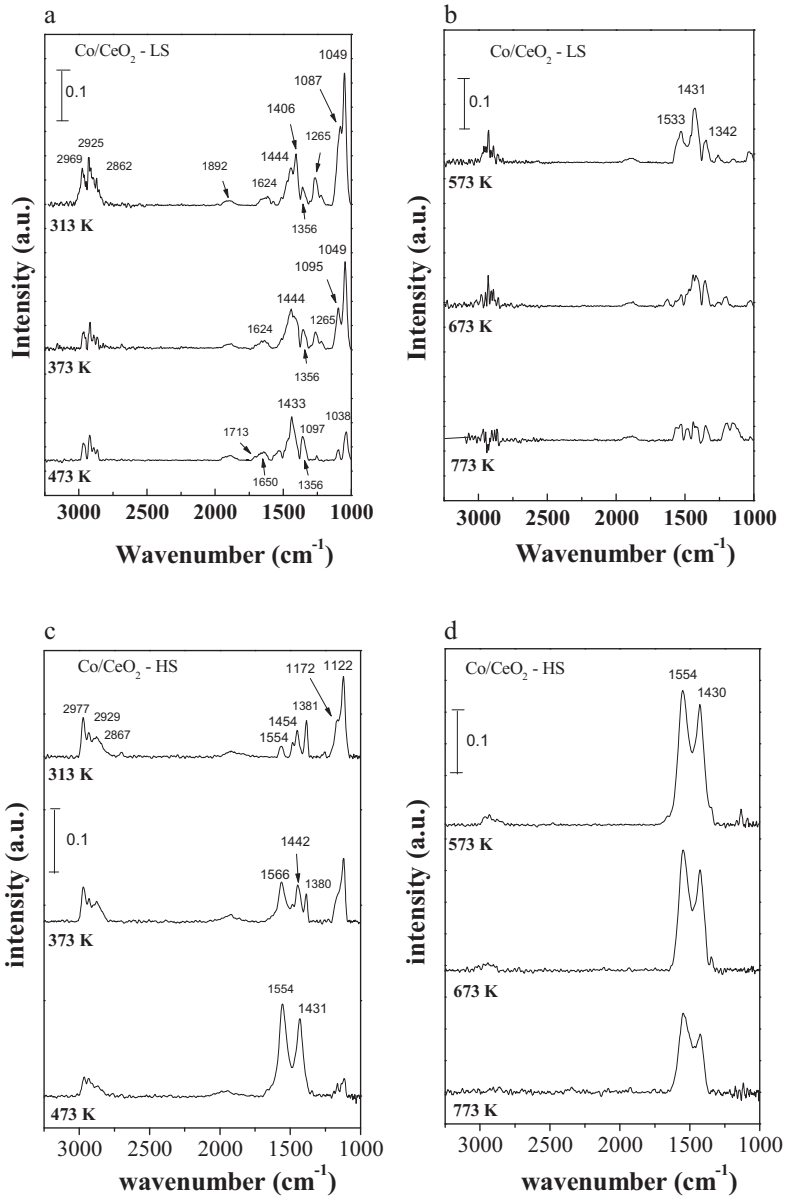

Fig. 1. DRIFTS spectra of adsorbed ethanol obtained on Co/CeO_2-LS and Co/CeO_2-HS catalysts at different temperatures.

face OH groups. Since the Co/CeO_2 catalyst was previously reduced at 1023 K, the acetate species were likely produced from the reaction between adsorbed acetaldehyde and surface OH groups. Song and Ozkan [7] also observed the presence of acetate species even at room temperature in the DRIFTS spectrum after ethanol adsorption over a Co/CeO_2 catalyst, which was attributed to the availability of oxygen from the ceria support.

Therefore, the DRIFTS spectra of adsorbed ethanol at room temperature indicate that Co/CeO_2-HS catalyst has a higher oxygen availability than Co/CeO_2-LS catalyst, which is in agreement with the OSC measurements. Evidence for the participation of oxygen from the support in the reaction mechanism becomes more clear when taking into account the spectra obtained at higher temperatures. Increasing the temperature to 373 and 473 K decreased the intensity of bands corresponding to ethoxy species for both catalysts. However, the decrease in the intensity of ethoxy bands was accompanied by a significant increase in the intensity of acetate species (1556–1554 and 1442–1431 cm^{-1}) for the Co/CeO_2-HS catalyst whereas, these bands were only observed at 573 K in the case of the Co/CeO_2-LS catalyst (Fig. 1b). Some authors [15,19,21] also obtained similar results in DRIFTS analysis of adsorbed ethanol for ceria supported metal catalysts. They suggested that ethoxy species can be decomposed to H_2, CH_4 and CO on metal particles at low temperatures. Therefore, these results indicate that increasing the reaction temperature favored the decomposition of ethoxy species to CH_4, CO and H_2 over Co/CeO_2-LS catalyst, whereas the ethoxy species were preferentially oxidized over Co/CeO_2-HS catalyst when the support was able to provide oxygen. At 773 K, bands were no longer detected on the Co/CeO_2-LS catalyst, while the bands assigned to acetate species were still present in the case of the Co/CeO_2-HS catalyst (Fig. 1b and d).

The DRIFTS spectra of Co/CeO_2-LS and Co/CeO_2-HS catalysts under the reaction mixture containing ethanol, water and oxygen are shown in Fig. 2a–d. For the Co/CeO_2-LS catalyst, even at room temperature, some acetate species are clearly present (ν_{as}(OCO) = 1558 cm^{-1}), indicating that in the presence of water and oxygen acetate formation is favored (Fig. 2a). In this case, O may be supplied via Type II OH groups from H_2O adsorption and O adatoms from O_2 adsorption. Besides this band, the spectrum at room temperature exhibits bands associated with ethoxy

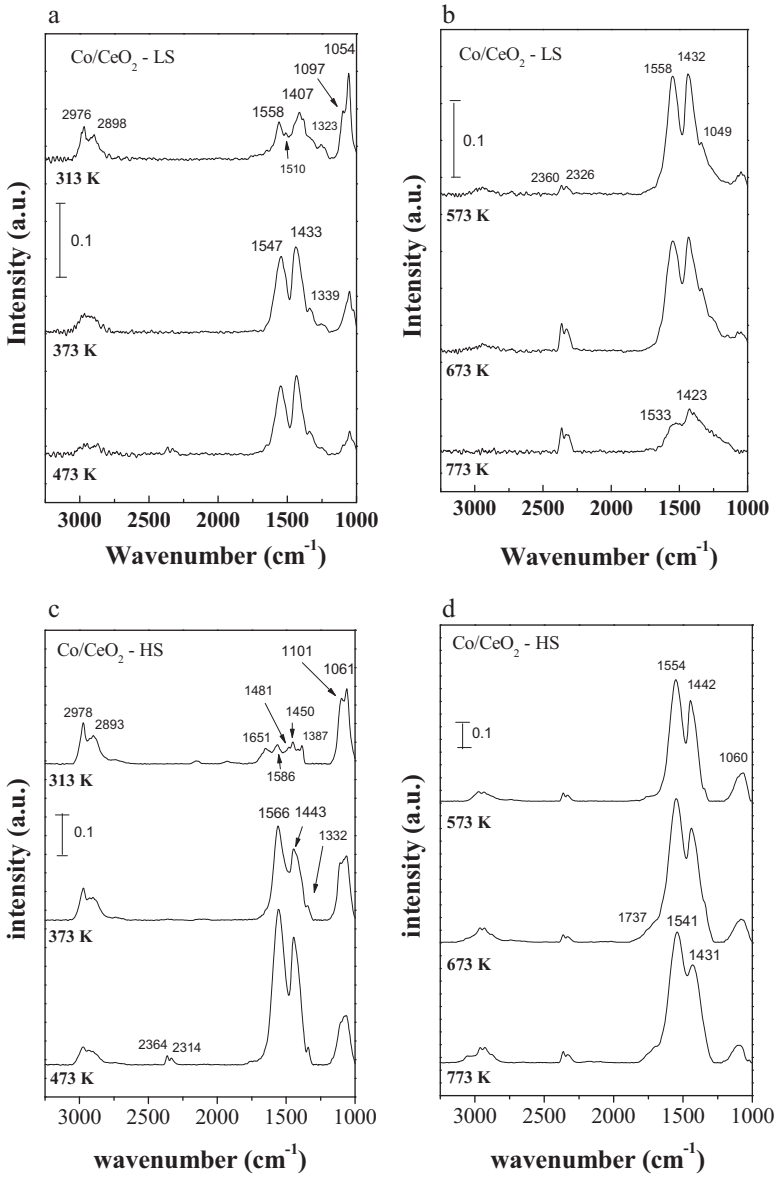

Fig. 2. DRIFTS spectra obtained on Co/CeO_2-LS and Co/CeO_2-HS catalysts at different temperatures and under the reaction mixture containing ethanol, water and oxygen (H_2O/ethanol ratio = 2.0; oxygen/ethanol ratio = 0.5).

species (1054, 1097 and 1407 cm^{-1}) and both ethoxy and acetate species (2976 and 2898 cm^{-1}). At 313 K, the DRIFTS spectrum of the Co/CeO_2-HS catalyst (Fig. 2c) is characterized by bands consistent with ethoxy species (1061, 1101, 1387 and 1450 cm^{-1}), acetyl species (1651 cm^{-1}) and acetate species (1586 cm^{-1}). A definitive assignment of acetyl species is difficult, since the water bending mode occurs in the same wavenumber range.

When both catalysts were heated to 373 and 473 K, the intensities of ethoxy bands clearly decreased, whereas those of acetate species (1547–1566 cm^{-1} and 1432–1443 cm^{-1}) increased mainly for the case of the Co/CeO_2-HS catalyst. At 473 K, the bands corresponding to gas phase CO_2 (~2360 cm^{-1}) were detected in the spectrum of Co/CeO_2-HS, whereas only a weak band appears in this region in the case of the Co/CeO_2-LS catalyst. Acetate species were preferentially decomposed to CH_4 and CO_2 via carbonate species preferentially over Co/CeO_2-HS [21].

Increasing temperature to the 573–773 K range led to a decrease in the intensities of bands corresponding to acetate species for Co/CeO_2-LS catalyst whereas those of Co/CeO_2-HS catalyst remained unchanged (Fig. 2b and d). At 773 K, only weak bands assigned to carbonate species were detected in the spectrum of Co/CeO_2-LS catalyst. On the other hand, the intensity of bands attributed to acetate species is still high for the Co/CeO_2-HS catalyst.

The DRIFTS results are in agreement with our earlier proposed mechanism for SR and OSR of ethanol over Pt/CeO_2 and Pt/CeO_2–ZrO_2 catalysts [19–21]. Ethanol adsorbs as ethoxy species, which may follow one of the two distinct pathways: (i) decomposition and production of CO, CH_4, and H_2 or (ii) dehydrogenation to acetaldehyde and acetyl species. The dehydrogenated species may undergo oxidation to acetate species. The addition of water and oxygen to the feed promoted the formation of acetate species. Water and oxygen also facilitated the acetate decomposition, resulting in the formation of methane, CO, and carbonate.

Therefore, the addition of water and oxygen to the feed promote the oxidation of ethoxy species to acetate species via reaction with support oxygen adatoms, as vacancies of the support could be continuously replenished by oxygen from the feed. This may involve dissociative adsorption of H_2O to form Type II bridging OH groups (i.e., without a formal change of oxidation state of cerium atoms involved – remaining Ce^{3+}) and/or reoxidation of ceria by O_2 to generate O adatoms (i.e., with formal change of oxidation state of cerium atoms involved to Ce^{4+}). Although this promoting effect is observed on both catalysts, the higher OSC of the high surface area ceria catalyst favors the oxidation of ethoxy species and the decomposition of acetate species.

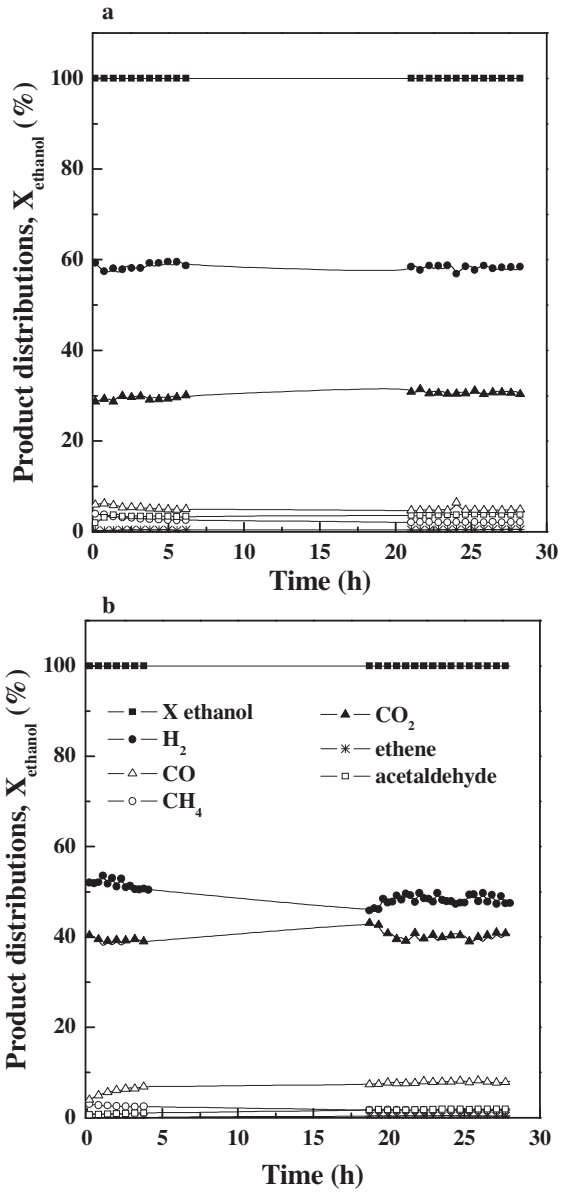

Fig. 3. Ethanol conversion ($X_{ethanol}$) and product distributions versus time on stream obtained during OSR under H_2O/ethanol molar ratio = 3.0 and O_2/ethanol molar ratio = 0.5 over (a) Co/CeO_2-LS catalyst; (b) Co/CeO_2-HS catalyst (mass of catalyst = 20 mg; $T_{reaction}$ = 773 K and residence time = 0.02 g s/mL).

3.2. OSR at 773 K over Co/CeO_2 catalysts

Fig. 3a and b shows the ethanol conversion and product distribution as a function of TOS obtained for Co/CeO_2–LS (Fig. 3a) and Co/CeO_2-HS (Fig. 3b) during OSR at 773 K. Complete ethanol conversion was observed for both catalysts during 30 h time on stream (TOS). H_2 and CO_2 were the main products formed, along with a small amount of acetaldehyde and CO, whereas no significant formation of ethylene was detected during the reaction. In addition, hydrogen selectivity was slightly higher while the CO_2 selectivity was lower in the case of the Co/CeO_2-LS catalyst.

The TG analyses of both catalysts after OSR did not reveal the presence of carbon deposits over the Co/CeO_2-HS catalyst, whereas a significant amount of carbon was formed over Co/CeO_2-LS catalyst (1.5 $mg_{carbon}/g_{catalyst}/h$).

According to the reaction mechanism proposed in the literature [19–21], the unbalance between the rate of decomposition of acetate species to CH_x species and the rate of desorption of CH_x species as CH_4 leads to the accumulation of carbon deposits, resulting in catalyst deactivation. The CH_x species may be further dehydrogenated to H and C. In the case of Co-based catalysts, this highly reactive carbon species will (a) react with O_2 (or H_2O) to produce CO_X species; (b) encapsulate the Co particle; or (c) diffuse through the Co crystallite and nucleate the growth of carbon filaments.

It has been reported in the literature that the support reducibility plays an important role on the stability of supported catalysts for different reactions such as CO_2 reforming of methane [22–24] and partial oxidation of methane [24–26]. It was suggested that carbon produced from the decomposition of CH_4 adsorbed on the metal particle becomes oxidized at the metal–support interface by oxygen from the support. These results strongly suggest that the catalyst stability during these reactions is related to the high oxygen storage capacity of the support. Therefore, the higher amount

of lattice oxygen near the metal particles promotes the mechanism of carbon removal from the metallic surface, which takes place at the metal–support interfacial perimeter.

Therefore, the higher oxygen/OH group mobility of high surface area ceria promotes the mechanism of carbon removal, which in turn contributes to the higher stability of Co/CeO_2-HS. In the presence of oxygen, support vacancies may be replenished, which keeps the cleaning mechanism operating efficiently. In the presence of steam, Type II bridging OH groups are activated at vacancies and can provide the oxygen necessary for the cleaning mechanism.

The addition of an excess of water or oxygen to the feed thus helps to clean the surface of the metal, keeping it active for a longer period of time. Therefore, the metal can remain active despite having a considerable amount of carbon deposited behind the particles, since the top surface will remain exposed to reactants and gas-phase intermediates. This can explain the stability of Co/CeO_2-LS even in the presence of carbon deposits.

4. Conclusions

Higher ceria surface area obtained by a new preparation technique enhanced stability by lowering the carbon deposition rate, as evidenced by TGA. Temperature programmed DRIFTS of adsorbed ethanol demonstrated the ability of ceria to donate oxygen, since ethanol decomposition products more readily formed acetate intermediate species. The oxygen may come from either vacancy-associated Type II bridging OH groups arising from the dissociative adsorption of water—whereby the cerium atoms involved with the OH groups are Ce^{3+}. Or, it may come from vacancy-associated O adatoms—whereby the cerium atoms involved with the O adatoms are Ce^{4+}. During OSR, support-O and/or support-OH assists in cleaning coke from Co, while oxygen vacancies are continuously replenished by O_2 (to form O adatoms) or H_2O (to form bridging OH groups), resulting in a continuous coke-removal mechanism.

Acknowledgements

This work received financial support of CTENERG/FINEP-01.04.0525.00. CAER acknowledges the Commonwealth of Kentucky for financial support.

References

[1] J. Llorca, P.R. de la Piscina, J. Sales, N. Homs, Chem. Commun. (2001) 641.
[2] P.D. Vaidya, A.E. Rodrigues, Ind. Eng. Chem. Res. 45 (2006) 6614.
[3] A. Haryanto, S. Fernando, N. Murali, S. Adhikari, Energy Fuels 19 (2005) 2098.
[4] L.V. Mattos, F.B. Noronha, J. Power Sources 152 (2005) 50.
[5] E.B. Pereira, N. Homs, S. Marti, J.L.G. Fierro, P.R. de la Piscina, J. Catal. 257 (2008) 206.
[6] J. Kugai, S. Velu, C. Song, M.H. Engelhard, Y. Chin, J. Catal. 238 (2006) 430.
[7] H. Song, U.S. Ozkan, J. Catal. 261 (2009) 66.
[8] J.C. Vargas, S. Libs, A.C. Roger, A. Kiennemann, Catal. Today 107 (2005) 417.
[9] H. Wang, Y. Liu, L. Wang, Y.N. Qin, Chem. Eng. J. 145 (2008) 25.
[10] J.M. Guil, N. Homs, J. Llorca, P.R. de la Piscina, J. Phys. Chem. B 109 (2005) 10813.
[11] A.E. Galetti, M.F. Gomez, L.A. Arrua, A.J. Marchi, M.C. Abello, Catal. Commun. 9 (2008) 1201.
[12] W. Cai, F. Wanga, E. Zhan, A.C. Van Veen, C. Mirodatos, W. Shen, J. Catal. 257 (2008) 96.
[13] H. Roh, A. Platon, Y. Wang, D.L. King, Catal. Lett. 110 (2006) 1.
[14] G.K. Chuah, S. Jaenicke, S.A. Cheong, K.S. Chan, Appl. Catal. A 145 (1996) 267.
[15] L.V. Mattos, F.B. Noronha, J. Catal. 233 (2005) 453.
[16] A. Yee, S.J. Morrison, H. Idriss, J. Catal. 191 (2000) 30.
[17] J. Raskó, A. Hancz, A. Erdohelyi, Appl. Catal. A 269 (2004) 13.
[18] P.V. Menacherry, G.L. Haller, J. Catal. 177 (1998) 175.
[19] S.M. de Lima, I.O. da Cruz, G. Jacobs, B.H. Davis, L.V. Mattos, F.B. Noronha, J. Catal. 257 (2008) 356.
[20] A. Erdohelyi, J. Raskó, T. Kecskés, M. Tóth, M. Dömök, K. Baán, Catal. Today 116 (2006) 367.
[21] S.M. de Lima, A.M. da Silva, U.M. Graham, G. Jacobs, B.H. Davis, L.V. Mattos, F.B. Noronha, Appl. Catal. A: Gen. 352 (2009) 95.
[22] S.M. Stagg-Williams, F.B. Noronha, G. Fendley, D.E. Resasco, J. Catal. 194 (2000) 240.
[23] F.B. Noronha, E.C. Fendley, R.R. Soares, W.E. Alvarez, D.E. Resasco, Chem. Eng. J. 82 (2001) 21.
[24] L.V. Mattos, E.R. de Oliveira, D.E. Resasco, F.B. Passos, F.B. Noronha, Fuel Process. Technol. 83 (2003) 147.
[25] L.V. Mattos, E.R. de Oliveira, P.D. Resende, F.B. Noronha, F.B. Passos, Catal. Today 77 (2002) 245.
[26] F.B. Passos, E.R. de Oliveira, L.V. Mattos, F.B. Noronha, Catal. Today 101 (2005) 23.